Improved stopped-flow time-resolved resonance Raman spectroscopy device for studying enzymatic reactions

Sachiko Yanagisawa,[a] Megha Subhash Deshpande,[b] Shun Hirota,[b*] Tatsuo Nakagawa[c] and Takashi Ogura [a,d*]

[a]*Graduate School of Life Science, University of Hyogo, RSC-UH Leading Program Center, Koto, Sayo-cho, Sayo-gun, Hyogo 679-5148, Japan*

[b]*Graduate School of Materials Science, Nara Institute of Science and Technology, 8916-5 Takayama-cho, Ikoma-city, Nara 630-0192, Japan*

[c]*UNISOKU Co., Ltd., Kasugano 2-4-3, Hirakata-city, Osaka 573-0131, Japan*

[d]*Picobiology Institute, Graduate School of Life Science, University of Hyogo, RSC-UH Leading Program Center, Koto, Sayo-cho, Sayo-gun, Hyogo 679-5148, Japan*

**Correspondence to: Takashi Ogura, Graduate School of Life Science, University of Hyogo, RSC-UH Leading Program Center, Koto, Sayo-cho, Sayo-gun, Hyogo 679-5148, Japan.*

Email: ogura@sci.u-hyogo.ac.jp

**Correspondence to: Shun Hirota, Graduate School of Materials Science, Nara Institute of Science and Technology, 8916-5 Takayama-cho, Ikoma-city, Nara 630-0192, Japan.*

Email: hirota@ms.naist.jp

Abbreviations

Mb: myoglobin

metMb: ferric myoglobin

RR: resonance Raman

Abstract

An improved stopped-flow resonance Raman spectroscopy device was constructed using a stopped-flow mixer with a dead time of 3 ms and a mixing volume of 0.1 mL. The device was tested using myoglobin, where the formation reaction of a high-valent heme species, ferryl-oxo heme, was monitored by time-resolved resonance Raman spectroscopy after mixing a ferric myoglobin solution with a hydrogen peroxide solution. The ferryl-oxo heme formation rate constant obtained by Raman spectroscopy is in good agreement with the rate constant obtained by conventional stopped-flow absorption spectroscopy for the same reaction under the same conditions. It is proved by these results that the present device is generally applicable to enzyme−substrate reactions with a significantly higher time resolution than previously reported.

Introduction

For detailed mechanistic studies of enzyme reactions, three dimensional structures of the enzymes are required. In addition, characterization of the enzyme reaction kinetics obtained by spectroscopy is indispensable. Stopped-flow[1] and mixed-flow techniques[2] are popular methods for initiating a chemical reaction by mixing two solutions. Stopped-flow has been mainly applied to absorption and fluorescence spectroscopy to study reaction kinetics with relatively small amounts of sample solutions. On the other hand, mixed-flow has been applied to resonance Raman (RR)[3-6] and EPR spectroscopies, and in these cases rich structural and electronic information can be obtained with the expense of relatively large amounts of sample solutions. Concerning RR spectroscopy, a simple mixer free jet device in air has been developed to avoid interference from quartz scattering,[7] whereas a circulating sample cell has been used to avoid localized sample heating.[8] By using a spectroelectrochemical circulating cell, the formal reduction potential of cytochrome *c* has been titrated and determined potentiometrically.[9] Stopped-flow RR spectroscopy has been applied to study organic oxidation reactions, which proceed through radical cations.[10] For protein conformational changes, a stopped-flow RR instrument with a time interval of 200 ms after mixing has been reported using a combination of a triple monochromator and an intensified

photodiode array detector as a Raman spectrophotometer,[11] whereas a stopped-flow apparatus for infrared spectroscopy has been reported.[12] Recent developments in a low noise CCD detector and a high efficiency notch filter to reduce Rayleigh scattering, combined with a single spectrograph, have led to the development of a significantly higher throughput Raman spectrophotometer. In the present study, we describe a stopped-flow RR device with a time resolution of 14 ms which is capable of providing time-resolved Raman spectra for the reaction of myoglobin (Mb) with hydrogen peroxide.

Experimental

Sample preparation

Horse skeletal muscle Mb was purchased from Sigma-Aldrich. A solution of H_2O_2 was prepared from a 30% (w/w) stock solution (Wako Pure Chemical Industries, Ltd., Japan), and its concentration was determined spectrophotometrically by quantitating the absorbance at 240 nm using the extinction coefficient of 43.6 $M^{-1}\cdot cm^{-1}$. All other chemicals were of the highest grade commercially available.

Stopped-Flow Absorption Measurements

The reaction of ferric Mb (metMb) (40 μM) in 5 mM potassium phosphate buffer, pH 7.0,

with H_2O_2 (50 mM) in the same buffer was initiated at 12 °C by mixing the two solutions at a 1:1 ratio using a commercially available stopped-flow apparatus (Unisoku Co., USP-SFM-S20) with customized mixing layers (Figure S1). The dead time was found to be 3 ms. The absorption spectra after the mixing were recorded with an interval of 25 ms up to 6 s for the 450–700 nm spectral region using a rapid-scan spectrophotometer (Unisoku Co., RSP-1000). Averaged spectra of 10 independent measurements were obtained.

Stopped-Flow RR Measurements

Figure S1 shows the schematics of the Raman observation cell assembled with a sample mixer. Multi-step mixing layers were used to maximize the mixing efficiency. The cell, integrated in the stopped-flow apparatus, was positioned at the sample point for the Raman dispersing spectrograph. Figure S2 shows a top view of the optical layout for Raman excitation and the collection optics at the cell. The excitation laser beam was vertically line-focused on the sample inside the cell using a cylindrical lens, and the excited RR scattering was collected at the right angle. Raman shifts were calibrated using the ethanol bands,[13] which were calibrated using the emission lines of neon.[14]

RR scattering was excited at 413.1 nm from a Kr^+ laser (Spectra Physics, 2060), dispersed by a spectrograph (SPEX, 750M, f = 750 mm, 1200 grooves/mm holographic grating), and

detected by a liquid-nitrogen cooled 1340×400 pixel CCD detector (Roper Scientific, Spec-10: 400B/LN, a full-frame CCD). A holographic notch filter (Kaiser Optical Systems, Inc.) was used to reduce Rayleigh scattering. Figure 1 depicts the time chart for external triggers, data readout delay, data readout time, syringe drive start time for mixing, syringe drive start delay, syringe drive moving time, and mixing completion time when the interval of the external trigger is 50 ms (20 Hz). The frame numbers (#1, #2, …) denote the accumulated light for the spectrum obtained by each trigger pulse at 50 ms intervals. The spectral data were treated using the software WinSpec (Princeton Instruments), and its “spectral mode” (line-binning mode) was used. In this mode, charges on 400 pixels in a vertical arrangement (perpendicular to the wavelength axis) were accumulated for respective 1340 rows, resulting in a spectrum having 1340 data points corresponding to the wavelength. A period of about 25 ms is required to transfer all of the data when 1340 rows of the detector were used. Since the charge transfer (data transfer) and charge accumulation by light exposure (data accumulation) take place simultaneously in the full-frame CCD, the readout delay must be set shorter than 25 ms, which corresponds to (trigger interval) – (data readout time). A pulse to start the syringe drive was supplied with a delay generator (Stanford Research Systems, DG535). By monitoring the mixing completion signal from the magnetic sensor of the device with an

oscilloscope, it was confirmed that the mixing is completed 60 ± 3 ms after the syringe drive starts to move. The timing to start the syringe drive for mixing the sample solutions (Mb solution and H_2O_2 solution) was adjusted so that the data accumulation of the first channel (Channel 1) starts to accumulate the data immediately after the mixing is completed. By taking into account the readout delay (20 ms) and trigger interval (50 ms), the syringe drive was set to start 10 ms after a trigger. The actual exposure time for each channel is equal to the trigger interval (50 ms). In Figure 1, frames #1 and #2 correspond to the data before mixing, frames #3 and #4 correspond to those during mixing, and frames #5 and above correspond to data after completion of the mixing. The delay time (Δt) is referenced to zero when the mixing is complete. The time window was different among channels and depended on the channel number. For example, the time window for Channel No. 1 was Δt = 0–50 ms, whereas that for Channel No. 1340 was 25–75 ms in spectrum #5. This is a consequence of the readout time of 25 ms. For the time window of each frame (spectrum), Δt of its Channel 1 is denoted. However, we also confirmed that the trigger interval could be shortened to 14.3 ms by limiting the number of vertical pixels to 10 and decreasing the readout time to less than 13.8 ms,

The reaction of metMb (40 μM) in 5 mM potassium phosphate buffer, pH 7.0, with H_2O_2

(50 mM) in the same buffer was initiated by mixing the two solutions at a 1:1 ratio using a stopped-flow device (Unisoku Co., USP-SFM-S20) at 12 ^{o}C. The mixing conditions for stopped-flow RR measurements were identical to those for stopped-flow absorption measurements. Experiments were repeated 15 to 57 times under each set of conditions with respect to the laser power, and the sum of the observed spectra for each time window was used for analysis. Single mixing required 0.1 mL for both the enzyme solution and the substrate solution.

Results and discussion

Time-resolved absorption change of Mb in the reaction with H_2O_2

Figure S3A shows the time-dependent absorption spectral change of metMb after mixing with H_2O_2. We note that the absorbance of the bands at 505 nm and 634 nm of metMb decrease with the reaction with H_2O_2, whereas the absorbance of the bands at 551 nm and 586 nm increase. The absorption bands at 551 nm and 586 nm of Mb have been attributed to the ferryl-oxo species, which possesses a protein radical (Compound II).[15,16] The ferryl-oxo species with a porphyrin π cation radical (Compound I) is highly reactive,[17] and its short lifetime prevents it from being observed under the present experimental conditions. Figure S3B shows a plot of the absorbance at 551 nm against time. Under the assumption that the

reaction obeys single exponential kinetics, the rate constant of the absorption change was found to be 3.4 ± 0.1 s^{-1} by least-square fitting. Figure S3B shows an excellent fit between experimental data and the assumed exponential curve.

Time-resolved RR spectral change of Mb in the reaction with H_2O_2

Figure 2 shows stopped-flow RR spectra generated in the reaction of metMb and H_2O_2 at a laser power of 20 mW for selected time windows. Figure S4 shows stopped-flow RR spectra generated in the same reaction at laser powers of 10 mW (A) and 56 mW (B). In all cases, the spin state marker (ν_2), the coordination number marker (ν_3), oxidation state marker (ν_4), vinyl bending ($\delta C_\beta C_a C_b$) and propionate bending ($\delta C_\beta C_c C_d$) modes are observed at 1562–1564 cm^{-1} (ν_2), 1483 cm^{-1} (ν_3), 1370–1372 cm^{-1} (ν_4), 438 cm^{-1} ($\delta C_\beta C_a C_b$) and 376–377 cm^{-1} ($\delta C_\beta C_c C_d$), respectively,[18] in the spectra of the time window from 0 to 50 ms. Since the RR spectra for the 0–50 ms time window of Figures 2 and S4 are essentially identical to that of metMb previously reported,[18] it is evident that the ferryl-oxo species is not yet generated at 0–50 ms. The ν_2, ν_3 and ν_4 bands shift to 1584–1586 cm^{-1}, 1507 cm^{-1} and 1376–1377 cm^{-1}, respectively, whereas the band intensities of the vinyl and propionate group bending modes became weaker with time.

Figure 3 shows expanded RR spectra in the 1340–1400 cm^{-1} region of Figures 2 and S4.

These spectra mainly exhibit the ν_4 mode. The spectra for the 10 mW laser power in Figure 3a show that the band at 1372 cm^{-1} at the time window of 0–50 ms exhibits a shift to 1377 cm^{-1} with time. Since the contribution of the 1377 cm^{-1} band is not negligible at 1372 cm^{-1}, but negligible at 1368 cm^{-1}, we analyzed the intensities at 1368 cm^{-1} and 1377 cm^{-1} to evaluate the time dependence of the ν_4 band shift. The change in position of the ν_4 band at 20 mW (Figure S4b) and 56 mW laser powers (Figure 3c) appear to be similar to the changes observed using the 10 mW laser power (Figure S4A) in that the band at 1372 cm^{-1} shows an upshift to 1377 cm^{-1} after mixing. However, it is noted that the band at 1377 cm^{-1} exhibits a decrease in intensity with time for laser powers of 20 mW and 56 mW (Figures 3b and 3c).

Figure 4 includes the Raman intensity plots against time for selected wavenumbers in Figures 2 and S4, including the propionate bending band at 376 cm^{-1} and the ν_4 bands at 1368 cm^{-1} and 1377 cm^{-1}. The rate constants of the intensity changes of selected RR wavenumbers were obtained under the assumption that the intensity changes obey single exponential kinetics based on least-square fitting with a rate constant of k (s^{-1}) in all cases except for the two cases discussed below. For the intensity fitting at 1377 cm^{-1} (20 mW and 56 mW), we assumed an increase and a decay in intensity with rate constants of k_1 and k_2, respectively. For the analysis of the 20 mW and 56 mW laser power data, we used the value of the 10 mW laser

power data as k_1 and obtained k_2. Similar rate constants in the range of 2.6–3.1 s^{-1} were obtained for the intensity decays at 376 cm^{-1} and 1368 cm^{-1} and intensity increase at 1377 cm^{-1}; an exponential curve is shown with a solid line on each plot in Figure 4. The rate constant obtained from the RR measurements is in good agreement with the rate constant obtained from stopped-flow absorption measurements (3.4 s^{-1}), and thus the process observed in the stopped-flow Raman measurements is interpreted as the formation of the ferryl-oxo Mb species. The second slower phase is seen when the two higher laser power conditions were employed to examine the 1377 cm^{-1} band (20 mW and 56 mW in Figure 4 as mentioned above). The second phase may be attributed to sample decomposition caused by photons and/or the temperature increase caused by the laser illumination, although it is not presently understood why decomposition occurs. However, when the H_2O_2 solution is replaced with a buffer solution (mixing metMb with buffer), there is no spectral change (data not shown) and the ensuing RR spectrum of this sample is identical to that of metMb.[18] The intensity decrease at 376 cm^{-1} and at 1368 cm^{-1} occurs simultaneously and is independent of the laser power, indicating that the wavenumber of the propionate band of the ferryl-oxo species shifts from 376 cm^{-1} to a different wavenumber.

Figure 5 shows the RR spectra of metMb (a) and ferryl-oxo Mb (b). The RR spectrum of

ferryl-oxo Mb is calculated by subtracting the RR spectrum of metMb from the spectrum obtained by summing the spectra for the time windows from 0 to 1300 ms of the 20 mW data, where an appropriate factor is used for the subtraction so that no negative peak appears in the difference spectrum. We limited the time window up to 1300 ms to avoid the effect of degradation on the resulting spectrum. Figure 5b exhibits the ν_{10}, ν_2, ν_3 and ν_4 bands at 1641 cm^{-1}, 1585 cm^{-1}, 1507 cm^{-1} and 1377 cm^{-1}, respectively, which are indicative of a high-valent low-spin heme.[19,20] In addition, the spectrum exhibits a band at 795 cm^{-1}, which is assignable to the $\nu_{Fe=O}$ (Fe=O stretching) mode.[20] All of these characteristics are consistent with the spectrum of the Compound II type ferryl-oxo species. Compound II is seen when measurements are obtained for three different laser power conditions. In the case of the higher laser powers of 20 mW and 56 mW, a decay in the intensity of the 1377 cm^{-1} band (the second phase with rate constant of k_2) is detectable as shown in Figure 4. The rate constants of the second phase depend on the laser power and have values of 0.6 s^{-1} and 1.1 s^{-1} for laser powers of 20 mW and 56 mW, respectively. However, there is no shift of the 1377 cm^{-1} band and only an intensity change was detected. These results indicate that higher laser power causes damage to the Compound II species. It is notable that no change in intensity is detectable for the 1377 cm^{-1} band after Compound II formation at the laser power of 10 mW (See Figure 4).

We also note that there is no change in the intensity of the 1371 cm^{-1} band originating from metMb even at the laser power of 56 mW for the static measurements (not shown).

Conclusions

In the present study, a stopped-flow RR device was constructed and tested. It was successfully applied to the reaction of metMb with hydrogen peroxide to generate Compound II of Mb with a measurement interval of 50 ms. To our knowledge, this represents the first report on measurement of the time-resolved RR spectra of Mb with consecutive time windows of 50 ms. The measurement interval could be set as narrow as 14 ms by limiting the pixel numbers of the CCD detector. The present stopped-flow RR device is promising for general investigations of enzyme−substrate reactions with higher time resolution than previously reported.

Acknowledgements

This study was supported by Grants-in-Aid for scientific research to T. O. (No. 26104532 and 15H00960) and S.H. (No. 26288080, 15H00945, and H1600839) from MEXT, Japan. S. Y. and T. O. are visiting scientists at RIKEN.

References

[1] B. Chance, *J. Franklin Inst.* **1940**, *229*, 455.

[2] H. Hartridge, F. J. W. Roughton, *Proc. Roy. Soc. London Ser. A* **1923**, *104*, 376.

[3] S. Takahashi, S. R. Yeh, T. K. Das, C. K. Chan, D. S. Gottfried, D. L. Rousseau, *Nat. Struct. Biol.* **1997**, *4*, 44.

[4] S. Yanagisawa, M. Horitani, H. Sugimoto, Y. Shiro, N. Okada, T. Ogura, *Faraday Discuss.* **2011**, *148*, 239.

[5] M. Tanaka, K. Matsuura, S. Yoshioka, S. Takahashi, K. Ishimori, H. Hori, I. Morishima, *Biophys. J.* **2003**, *84*, 1998.

[6] L. R. Sans Cartier, A. C. Storer, P. R. Carey, *J. Raman Spectrosc.* **1988**, *19*, 117.

[7] C. Varotsis, G. T. Babcock, *Methods Enzymol.* **1993**, *226*, 409.

[8] W. H. Woodruff, T. G. Spiro, *Appl. Spectrosc.* **1974**, *28*, 74.

[9] J. L. Anderson, J. R. Kincaid, *Appl. Spectrosc.* **1978**, *32*, 356.

[10] J. C. Merlin, J. L. Lorriaux, R. E. Hester, *J. Raman Spectrosc.* **1981**, *11*, 384.

[11] T. Uno, Y. Nishimura, M. Tsuboi, *Biochemistry* **1984**, *23*, 6802.

[12] A. J. White, K. Drabble, C. W. Wharton, *Biochem. J.* **1995**, *306 (Pt 3)*, 843.

[13] Wavenumbers of 433.5, 883.3, 1051.6, 1095.2, 1275.6, and 1453.7 cm^{-1} were used for the corresponding peaks. H. Hamaguchi, A. Hirakawa, Y. Ozaki, in *Raman spectroscopy*, (Eds: H. Hamaguchi, A. Hirakawa), Spectroscopical Society of Japan, Scientific Societies Press, Tokyo, **1988**, p 217.

[14] K. Burns, K. B. Adams, J. Longwell, *J. Opt. Soc. Am.* **1950**, *40*, 339.

[15] N. K. King, M. E. Winfield, *J. Biol. Chem.* **1963**, *238*, 1520.

[16] C. W. Fenwick, A. M. English, *J. Am. Chem. Soc.* **1996**, *118*, 12236.

[17] T. Egawa, H. Shimada, Y. Ishimura, *J. Biol. Chem.* **2000**, *275*, 34858.

[18] S. Hu, K. M. Smith, T. G. Spiro, *J. Am. Chem. Soc.* **1996**, *118*, 12638.

[19] J. Terner, V. Palaniappan, A. Gold, R. Weiss, M. M. Fitzgerald, A. M. Sullivan, C. M. Hosten, *J. Inorg. Biochem.* **2006**, *100*, 480.

[20] A. J. Sitter, C. M. Reczek, J. Terner, *Biochim. Biophys. Acta* **1985**, *828*, 229.

Supporting information

Additional supporting information may be found in the online version of this article at the publisher's website.

Figure legends

Figure 1. Time chart for external triggers, data readout delay, data readout time, syringe drive start time for mixing, syringe drive start delay, syringe drive moving time, and mixing completion time. The case for trigger intervals of 50 ms is shown. CCD was used with full-frame mode (1340×400 pixels) (See text in detail).

Figure 2. Stopped-flow resonance Raman spectra at selected time windows. The time window for each spectrum is shown on the right hand side. Data with consecutive time windows from 0 to 4650 ms were obtained at 50 ms intervals, and the spectra with selected time windows are shown. The laser power was adjusted to 20 mW at the sample point. Concentrations of metMb and H_2O_2 were 20 μM and 25 mM, respectively, after mixing.

Figure 3. Expanded RR spectra in the ν_4 wavenumber region for Figures 2 and S4 with laser powers of 10 mW (a), 20 mW (b) and 56 mW (c), respectively.

Figure 4. The time courses of the normalized Raman intensities at 376 cm^{-1} (a), 1368 cm^{-1} (b) and 1377 cm^{-1} (c) at three specified laser powers (10, 20 and 56 mW). Raman intensities are plotted using red, blue and green dots for the data with laser powers of 10 mW, 20 mW and 56 mW, respectively. Least-square-fitted exponential curves are shown in black lines for the data with laser power of 10 mW and in red lines for the data with laser powers of 20 mW and 56

mW. The obtained rate constants are also depicted.

Figure 5. Resonance Raman spectra of metMb (a) and ferryl-oxo Mb (b) (See text in detail).

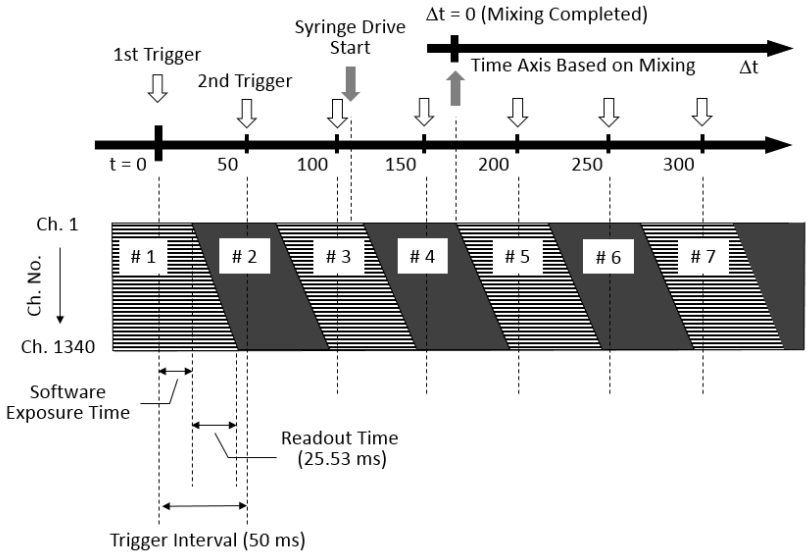
Δt = 0 (Mixing Completed)
Syringe Drive Start
1st Trigger
2nd Trigger
Time Axis Based on Mixing
Δt
t = 0
50
100
150
200
250
300
Ch. 1
Ch. No.
Ch. 1340
1
2
3
4
5
6
7
Software Exposure Time
Readout Time (25.53 ms)
Trigger Interval (50 ms)

Figure 1.

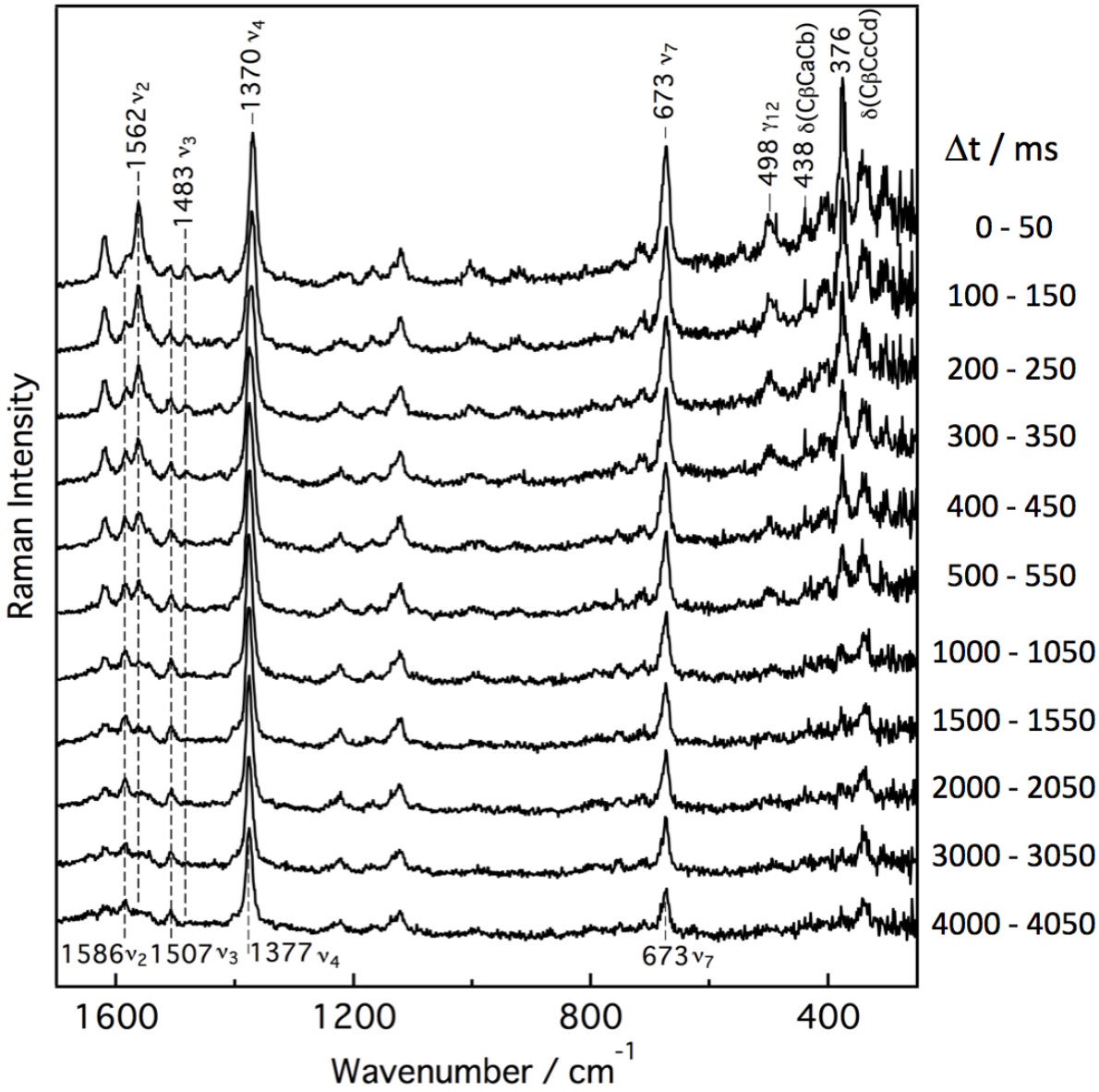
1562 ν2
1483 ν3
1370 ν4
673 ν7
498 γ12
438 δ(CβCaCb)
376
δ(CβCcCd)
Δt / ms
0 - 50
100 - 150
200 - 250
300 - 350
400 - 450
500 - 550
1000 - 1050
1500 - 1550
2000 - 2050
3000 - 3050
4000 - 4050
1586ν2 1507ν3 1377ν4
673ν7
Raman Intensity
1600
1200
800
400
Wavenumber / cm-1

Figure 2.

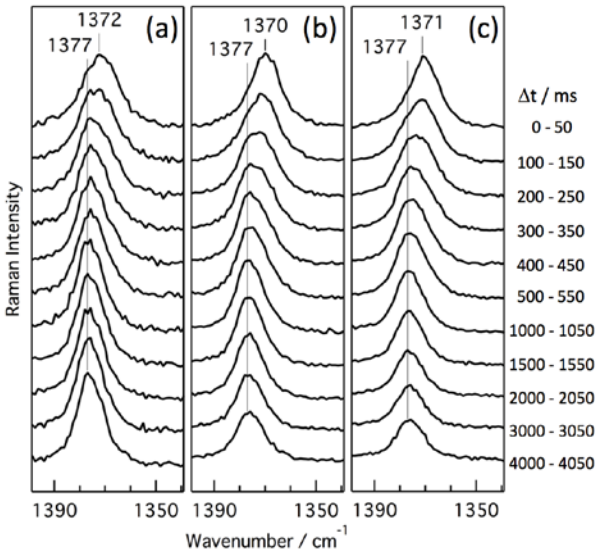
1372
1377
(a)
1370
1377
(b)
1371
1377
(c)
Δt / ms
0 - 50
100 - 150
200 - 250
300 - 350
400 - 450
500 - 550
1000 - 1050
1500 - 1550
2000 - 2050
3000 - 3050
4000 - 4050
Raman Intensity
1390
1350
1390
1350
1390
1350
Wavenumber / cm-1

Figure 3.

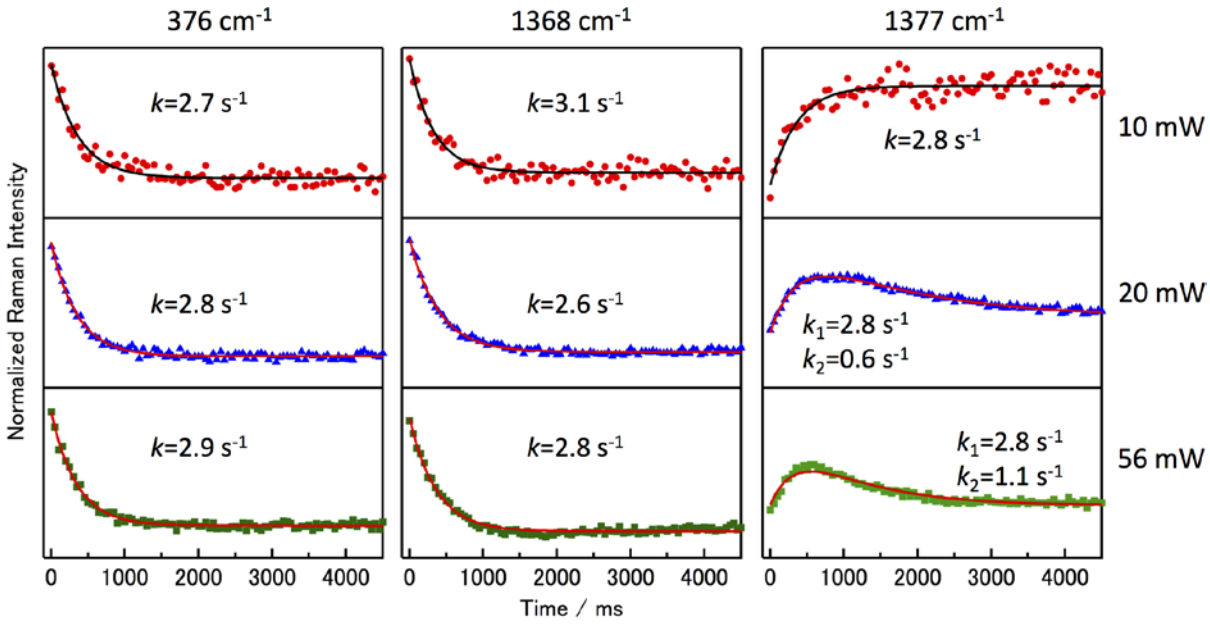
376 cm-1
1368 cm-1
1377 cm-1
k=2.7 s-1
k=3.1 s-1
k=2.8 s-1
10 mW
k=2.8 s-1
k=2.6 s-1
k1=2.8 s-1
k2=0.6 s-1
20 mW
k=2.9 s-1
k=2.8 s-1
k1=2.8 s-1
k2=1.1 s-1
56 mW
Normalized Raman Intensity
0
1000
2000
3000
4000
Time / ms

Figure 4.

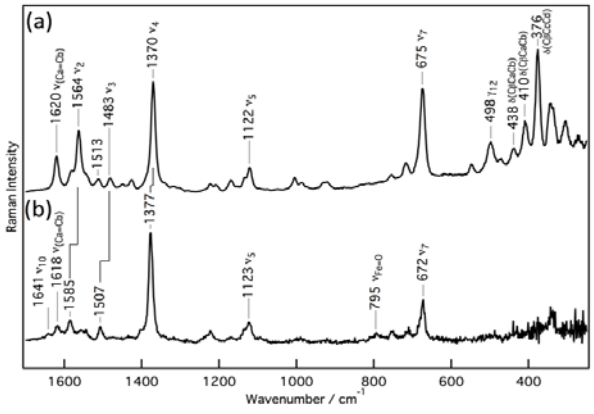
(a)
(b)
Raman intensity
1620 ν(Ca=Cb)
1564 ν2
1513
1483 ν3
1370 ν4
1122 νs
675 ν7
498 t12
438 δ(CpCaCb)
410 δR(CpCaCb)
376 δ(CaCbCb)
1641 ν19
1618 ν(Ca=Cb)
1585
1507
1377
1123 νs
795 νFe=O
672 ν7
1600
1400
1200
1000
800
600
400
Wavenumber / cm-1

Figure 5.

TOC

An improved stopped-flow resonance Raman spectroscopy device was constructed using a stopped-flow mixer with a dead time of 3 ms and a mixing volume of 0.1 mL. The device was tested using myoglobin, where the formation reaction of a high-valent heme species, ferryl-oxo heme, was monitored by time-resolved resonance Raman spectroscopy after mixing a ferric myoglobin solution with a hydrogen peroxide solution. The present device is generally applicable to enzyme−substrate reactions with a significantly higher time resolution than previously reported.

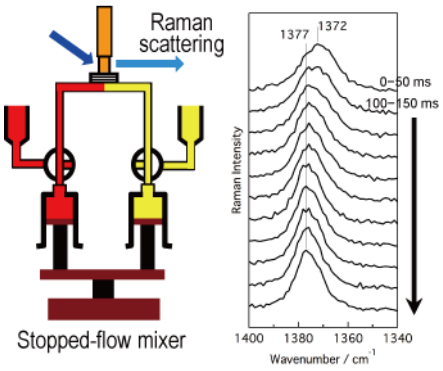

Supporting Information

for

Improved stopped-flow time-resolved resonance Raman spectroscopy device for studying enzymatic reactions

Sachiko Yanagisawa,[a] Megha Subhash Deshpande,[b] Shun Hirota,[b*] Tatsuo Nakagawa[c] and Takashi Ogura [a,d*]

[a]*Graduate School of Life Science, University of Hyogo, RSC-UH Leading Program Center, Koto, Sayo-cho, Sayo-gun, Hyogo 679-5148, Japan*

[b]*Graduate School of Materials Science, Nara Institute of Science and Technology, 8916-5 Takayama-cho, Ikoma-city, Nara 630-0192, Japan*

[c]*UNISOKU Co., Ltd., Kasugano 2-4-3, Hirakata-city, Osaka 573-0131, Japan*

[d]*Picobiology Institute, Graduate School of Life Science, University of Hyogo, RSC-UH Leading Program Center, Koto, Sayo-cho, Sayo-gun, Hyogo 679-5148, Japan*

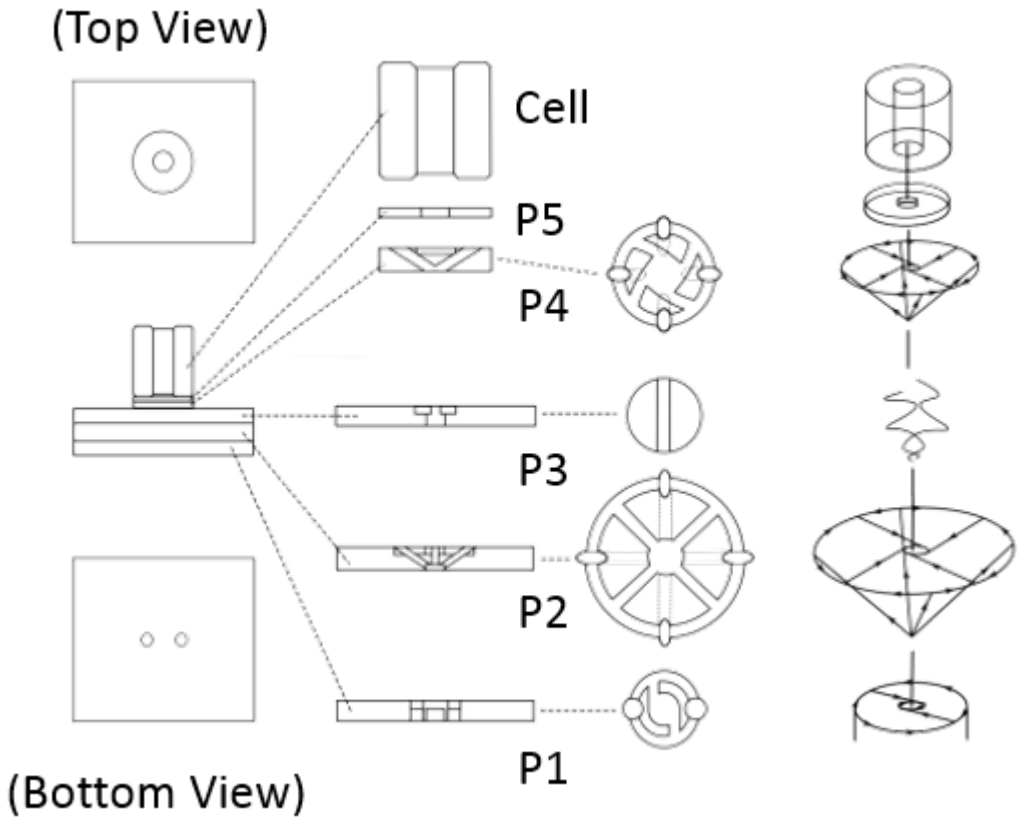

Figure S1. Schematic views of the Raman observation quartz cylinder cell with multi-step mixing layers. Left column, assembled state of the cell; middle column, disassembled state into 5 layer pieces (P1 – P5) of the cell; right column, illustration of the sample flow. Arrows indicate the direction of the solution flow. The inner and outer diameters of the cell are 2 and 6 mm, respectively. The mixing layers are made from machinable glass ceramic MACOR (Corning Inc., NY), and glued together with EPO-TEK H74 (Epoxy Technology Inc., MA). The width and depth of P1 – P3 are 16 and 12 mm, respectively, and the thicknesses are 1.5, 2 and 1.5 mm, respectively. The diameter of P4 and P5 is 6 mm, and the thicknesses are 1.5 and 0.5 mm, respectively.

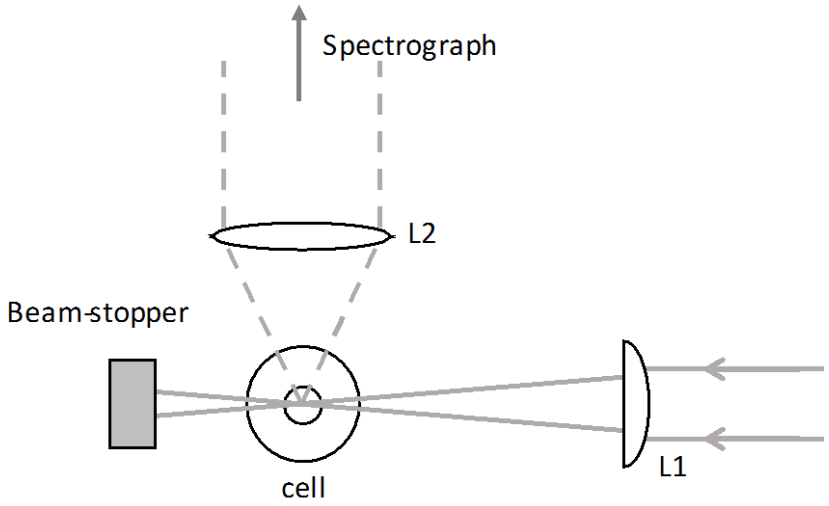

Figure S2. Optical layout of Raman optics (Top view). L1 is a cylindrical lens with f = 200 mm. L2 is a camera lens with f = 50 mm.

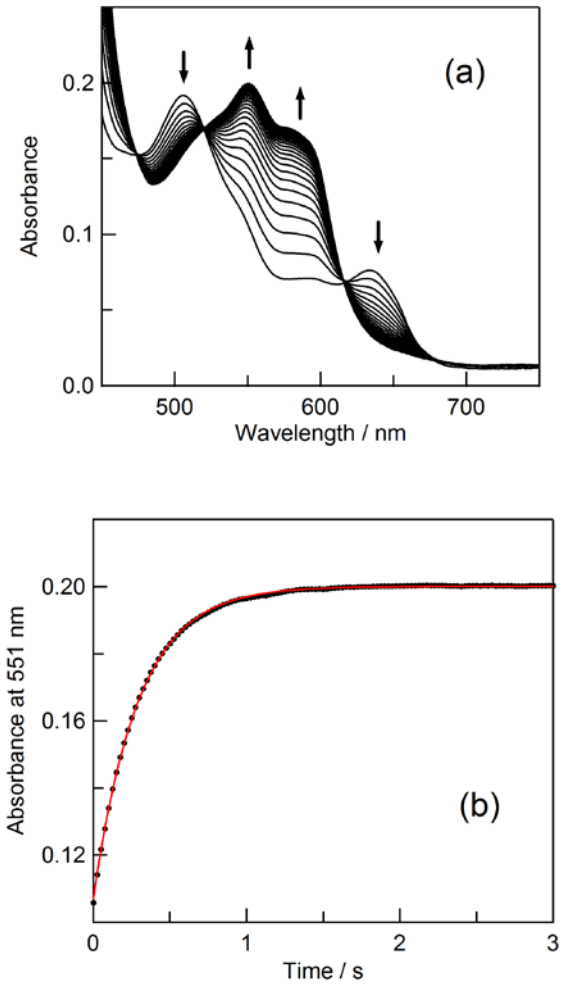

Figure S3. Time-resolved absorption spectra for the reaction of MetMb with H_2O_2. (A) Spectral changes with an interval of 50 ms up to 3 s is shown. (B) Absorbance change at 551 nm (black dots), together with a least-square-fitted exponential curve (red line). The directions of the 4 arrows in (A) indicate the absorbance decrease at 505 nm, increase at 551 nm, increase at 586 nm and decrease at 634 nm with the ascending order of wavelength value. The concentrations of metMb and H_2O_2 were 20 μM and 25 mM, respectively, after mixing.

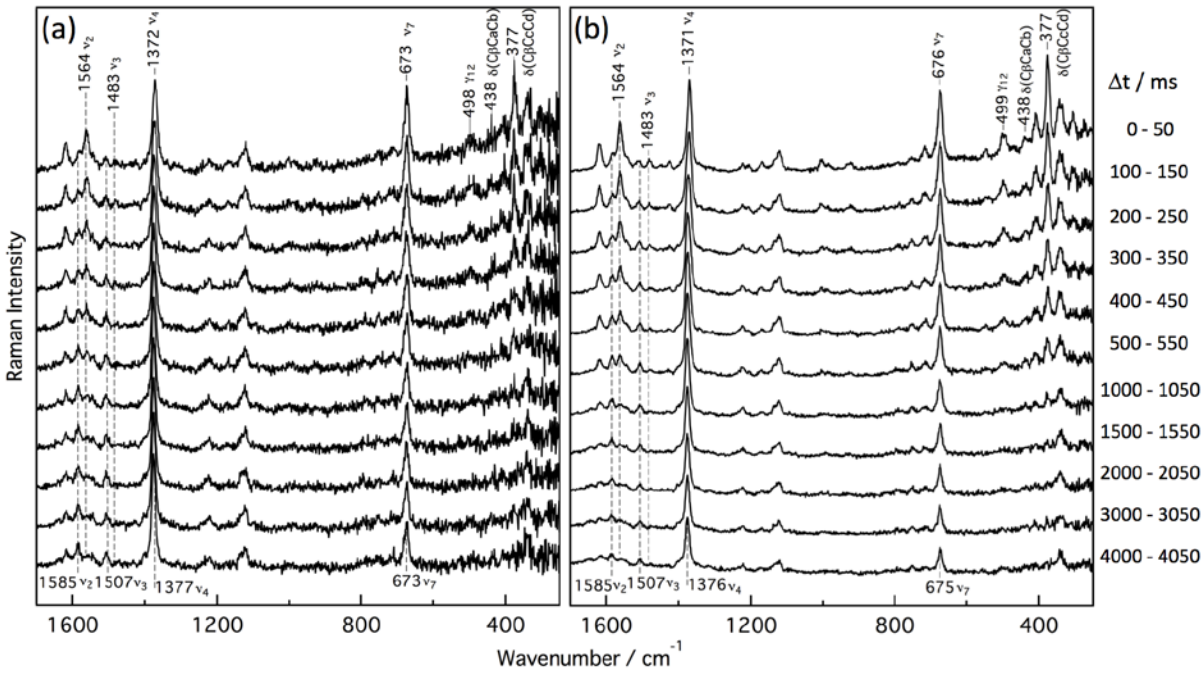

Figure S4. Stopped-flow resonance Raman spectra at selected time windows. The time window for each spectrum is shown in the right hand side. Data with a consecutive time window from 0 to 4650 ms were obtained at 50 ms intervals, and the spectra with selected time windows are shown. The laser power was adjusted to 10 mW (a) and 56 mW (b) at the sample point. Concentrations of metMb and H_2O_2 were 20 μM and 25 mM, respectively, after mixing.